

Precision neutron-diffraction study of the high- T_c superconductor $\text{HgBa}_2\text{CuO}_{4+\delta}$

V. L. Aksenov, A. M. Balagurov,* V. V. Sikolenko, and V. G. Simkin
JINR, FLNP, 141980 Dubna, Russia

V. A. Alyoshin, E. V. Antipov, A. A. Gippius, D. A. Mikhailova, and S. N. Putilin
Moscow State University, 119899 Moscow, Russia

F. Bouree
LLB, 91191 Gif-sur-Yvette, France

(Received 31 July 1996)

A neutron-diffraction study of $\text{HgBa}_2\text{CuO}_{4+\delta}$ structure and its dependence on extra oxygen content for δ between 0.06 and 0.19 has been carried out with four pure samples using high-resolution TOF and $\lambda=\text{const}$ diffractometers at room temperature and $T=8$ K. Sample characterization was done by measuring ac susceptibility, x-ray and EPR spectra, and by iodometric titration. A detailed analysis of atomic structure and the occupancy factors of mercury and oxygen was performed and showed the stoichiometric cation content. Extra oxygen was found only in the $(1/2, 1/2, 0)$ position of the basal plane. T_c varied parabolically with δ and exhibited a maximum of 98 K at $\delta \approx 0.12$. The data obtained can be considered as evidence of the conventional anion doping mechanism with 2δ holes per CuO_2 layer. [S0163-1829(97)01506-3]

I. INTRODUCTION

One of the obstacles encountered in investigation of the mechanisms of high- T_c superconductivity is connected with fair complexity of the crystal structure of copper oxides and diversity of their structural defects. This is the reason why mercury-bearing superconducting copper mixed oxides with general formulas of $\text{HgBa}_2\text{Ca}_{n-1}\text{Cu}_n\text{O}_{2n+2+\delta}$ are attractive to the investigation of the relationship between structure and superconducting properties. These compounds have a remarkably high critical temperature and relatively simple crystal structures. The simplicity of their structures is caused by the absence of a mismatch between the layers of (CuO_2) , (BaO) , (Ca) , and (HgO_δ) alternating along the c axis of the unit cell.¹ Moreover, the first member of the homologous series $\text{HgBa}_2\text{CuO}_{4+\delta}$ (designated Hg-1201) has practically none of the layer stacking faults along the c axis existing in other members of the series² that introduce systematic errors into the refinement of these layered structures based on diffraction data. As a result, Hg-1201 can be considered as one of the most convenient compounds for the structural studies of high- T_c materials.

The simplicity of the $\text{HgBa}_2\text{CuO}_{4+\delta}$ structure created great interest in investigating the structure of this compound with different extra oxygen contents (δ), which influence the transition temperature to the superconducting state (T_c).³⁻¹² It should be mentioned that the presence of only one type of oxidizing fragment in the $\text{HgBa}_2\text{CuO}_{4+\delta}$ structure, namely, Cu atoms in (CuO_2) layers, provides a paraboliclike dependence of T_c on the extra oxygen content, which determines the hole concentration in the conducting band (p). Assuming the formal valence of the atoms to be $V_{\text{Hg}}=V_{\text{Ba}}=+2$ and $V_{\text{O}}=-2$, one can calculate the hole concentration $p=2\delta$ for Hg-1201. The results of iodometric titration, to determine the formal copper valence (V_{Cu}),^{8,10,12} showed that the maximum transition temperature is realized at $V_{\text{Cu}}=+2.16$ and T_c

drops when the oxygen content shifts to either sides of this optimal value. This result is in a good agreement with experimental data obtained for other Cu-containing superconductors.¹³⁻¹⁵ Based on this data, the universal parabola equation for the dependence of T_c on p was proposed:¹⁴

$$T_c/T_{c,\text{max}} = 1 - 82.6 (p - 0.16)^2. \quad (1)$$

According to this equation, the maximum transition temperature is realized at a hole concentration corresponding to the formal copper valence of $V_{\text{Cu}}=+2.16$.

Recently, several structural investigations of $\text{HgBa}_2\text{CuO}_{4+\delta}$ based on powder neutron-diffraction experiments, were done.⁴⁻⁹ In general, there is good agreement between the refined structural parameters, but, at the same time, there are severe discrepancies concerning the Hg and interstitial oxygen positions and occupancies. As an example, the occupancies of the O3 position (the center of the Hg layer) obtained in Refs. 4-9 for samples with close T_c are listed in Table I. Calculations of the formal copper valence based on some of these data lead to numbers considerably different from the optimal value determined by Eq. (1).

In the first structural paper on Hg-1201, the extra oxygen was put in the center of the basal plane only,³ but later in

TABLE I. Oxygen content in the O3 position (the center of Hg layer) in Hg-1201 structure with T_c close to $T_{c,\text{max}}$ as was obtained in neutron-diffraction experiments.

| Ref. | 4 | 5 ^a | 6 | 7 ^a | 9 |
|----------------|-----------|----------------|---------|----------------|---------|
| T_c , K | 94 | 95 | 95 | 97 | 94 |
| $n(\text{O}3)$ | 0.063(14) | 0.059(6) | 0.18(1) | 0.112(8) | 0.10(1) |

^aAn additional position for oxygen was found.

Refs. 5 and 7 were found partial substitution of Hg atoms by copper (7 and 20 %) and the appearance of additional interstitial oxygen near the perovskite oxygen position (middle of the edge) bonded to these Cu atoms. That this substitution takes place, though probably under specific synthetic conditions, and complicates the interpretation of the T_c vs p relationship because of the additional Cu atom (in the Hg position) which can change the oxidation state.

For the fitting between neutron and thermoelectric power data of Hg-1201 samples with different δ values, a formal charge close to -1 for the interstitial oxygen atom was suggested.^{6,11} This oxidation state, however, was only found earlier in the peroxide group.¹⁶ The existence of isolated O^{-1} ions in the Hg-1201 structure at such long distances from the cations ($d_{\text{Hg-O3}}$ and $d_{\text{Ba-O3}} > 2.7 \text{ \AA}$) is doubtful because of the high chemical activity of the O^{-1} ions due to the unpaired electron.

Mercury cations can be partially replaced not only by copper but also by carbonate groups, as was shown for the Hg-1201 and Hg-1223 samples obtained by the high-pressure technique.^{8,17} It should be mentioned that in this case isovalent substitution is realized because $[\text{HgO}_2]^{2-}$ dumbbells are replaced by $[\text{CO}_3]^{2-}$ groups that do not change the hole concentration. But the presence of the additional oxygen atoms bonded to carbon can lead to the higher oxygen concentration found from neutron data. Thus, in studying Hg oxides, we are faced with a typical high- T_c materials problem when it is not quite clear what is under investigation, compound or sample.

In this paper, using our previous experience, we have tried to synthesize a series of monophasic Hg-1201 samples with different δ for systematic investigation of the occupation of the interstitial oxygen position (or positions) as well as the problem of partial occupation of Hg position or deficiency of this position. A sample characterization was done by measuring ac susceptibility, x-ray spectra, ICP-AES element analysis for Hg, Ba, and Cu, and by iodometric titration. Important information was obtained by measuring EPR spectra. The main part of the experiments was carried out with the high-resolution diffractometers at the IBR-2 high-flux pulsed neutron source in Dubna and at the steady-state reactor Orphee in Saclay. Due to the high-quality diffraction data we were able to obtain the precise structural information from the Rietveld refinement and additionally to calculate scattering density maps to reveal the important details of the structure.

II. SYNTHESIS AND SAMPLE CHARACTERIZATION

Four samples of $\text{HgBa}_2\text{CuO}_{4+\delta}$ (A, B, C, and D) were synthesized from stoichiometric mixtures of $\text{Ba}_2\text{CuO}_{3+x}$ and HgO according to methods described in Ref. 12. The synthesis was carried out at $800 \text{ }^\circ\text{C}$ for 6 h in evacuated silica tubes in a two-temperature gradient furnace. Samples A, C, and D were annealed at controlled partial oxygen pressures, created by a mixture of $\text{Co}_3\text{O}_4/\text{CoO}$ and $\text{CuO}/\text{Cu}_2\text{O}$ oxides (for sample D) situated in the hotter part of the tubes. Samples A ($m=2.09 \text{ g}$) and C ($m=1.93 \text{ g}$) were obtained at $p(\text{O}_2)=0.15 \text{ bar}$; sample D ($m=1.84 \text{ g}$) was obtained at $p(\text{O}_2)=0.0012 \text{ bar}$. In the case of sample B ($m=2.05 \text{ g}$), an additional pellet of $\text{Ba}_2\text{CuO}_{3+x}$ was placed in the hot part of

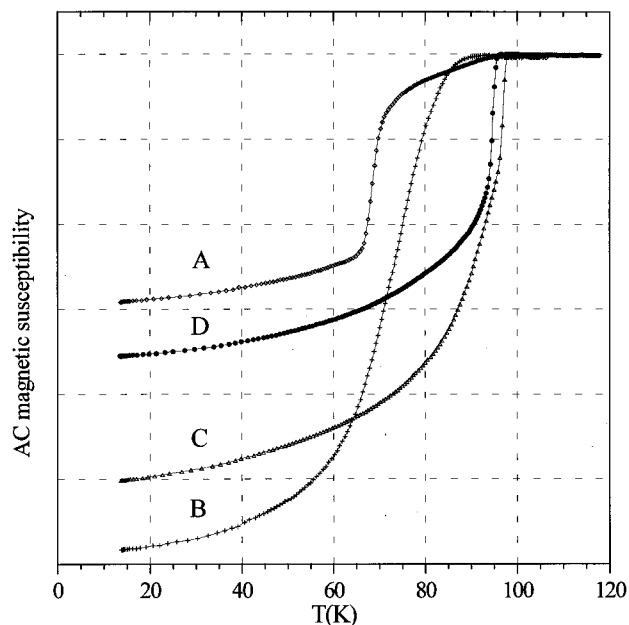


FIG. 1. ac magnetic susceptibility for samples A–D as measured at 27 Hz in a magnetic field of 1 Oe.

the tube ($820 \text{ }^\circ\text{C}$) to decrease the partial mercury pressure. Samples thus synthesized were then annealed for more than 24 h in a flow of oxygen at $250 \text{ }^\circ\text{C}$ (C and D), argon at $350 \text{ }^\circ\text{C}$ (A), and under oxygen pressure as high as 90 bars at $250 \text{ }^\circ\text{C}$ (B).

Phase composition of the samples was determined from x-ray powder data (Guinier FR-552 focusing camera, $\text{Cu}_{K\alpha 1}$ radiation, $\lambda=1.54056 \text{ \AA}$, Ge internal standard). Samples A, B, C contained only the Hg-1201 phase, with the exception of traces of the starting $\text{Ba}_2\text{CuO}_{3+x}$ phase found with the main Hg-1201 phase in sample D.

To check chemical composition of one of the monophasic samples obtained at the same conditions and with cell parameters close to sample C, its full chemical analysis was carried out in MPI (Stuttgart). Hg, Ba, and Cu concentrations were determined by the ICP-AES technique, and total oxygen content by the “solid-state hot-gas” method (crystal SiO_2 as an internal standard). It gave good agreement with a stoichiometric cation composition: $\text{Hg}_{0.99(1)}\text{Ba}_{2.00(1)}\text{Cu}_{0.97(1)}\text{O}_{4.03(6)}$.

The formal oxidation state of copper was determined by iodometric titration, described in Ref. 18. Based on the iodometric data, the formal charges of copper atoms were $V_{\text{Cu}}=+2.02$ (sample A), $+2.25$ (B), $+2.16$ (C) with statistical errors of 0.02. The formal oxidation states of the other atoms was assumed to be standard: $V_{\text{Hg}}=V_{\text{Ba}}=+2$ and $V_{\text{O}}=-2$. In this case, the chemical formulas of the studied compounds can be written as $\text{HgBa}_2\text{CuO}_{4.01(1)}$ (A), $\text{HgBa}_2\text{CuO}_{4.13(1)}$ (B), $\text{HgBa}_2\text{CuO}_{4.08(1)}$ (C). Sample D was not investigated by this method due to the presence of impurities which were detected by x rays. The oxygen content of all samples including sample D was refined then in a neutron-diffraction experiment.

ac magnetic susceptibility measurements were carried out in the temperature range 12–120 K with an external field of $H_0=1 \text{ Oe}$ at a frequency of 27 Hz. The dependence of $\chi(T)$ for all samples is shown in Fig. 1. Since the beginning of the

transitions for samples *A* and *B* is not sharp, probably due to an inhomogeneous distribution of the extra oxygen, the temperature of the sharp drop in χ was assumed as the transition temperature, namely, $T_c = 71$ K (*A*), 83 K (*B*), 98 K (*C*) and 96 K (*D*).

Measurements of EPR spectra for samples *A* and *C* were performed on the 3-cm range E-4 (Varian) EPR spectrometer. Powder patterns with $\sim 1\text{-}\mu\text{m}$ particle sizes were used for the measurements. This allowed the skin effect on the EPR spectra to be excluded, because of the thickness of the skin layer at the working frequency of the spectrometer (9.18 GHz), for a sample with a resistivity of several mOhm cm is about 10–20 μm . EPR spectra were measured at room temperature in a range of magnetic fields up to 4000 Gs, at microwave frequency power of 20 mW, with modulation amplitude of magnetic field of 8 Gs and frequency modulation of 100 kHz.

III. NEUTRON DIFFRACTION

Neutron-diffraction experiments were performed with the high-resolution Fourier diffractometer¹⁹ (HRFD) at the IBR-2 pulsed reactor in Dubna and with the constant wavelength diffractometer 3T2 at the Orphee reactor in Saclay. The HRFD diffractometer is a time-of-flight (TOF) correlation spectrometer using a fast-Fourier chopper for modulating the intensity of the incident neutron beam and the RTOF method for gathering scattered neutrons. The HRFD d -spacing resolution depends on the frequency of the intensity modulation, and in the experiments with $\text{HgBa}_2\text{CuO}_{4+\delta}$ it was close to $\Delta d/d = 0.0015$. The 3T2 ($\lambda = 1.227$ Å) is a high-resolution powder diffractometer ($\Delta d/d$ is close to 0.003 at the minimum of the resolution curve for 10' collimator before sample), equipped with 20 ^3He detectors.

A cylindrical, 5-mm-diam, Ti-Zr sample holder without coherent scattering was used to hold the Hg-1201 powder. Diffraction patterns were measured with HRFD for samples *A–D* at room temperature and for sample *B* at $T = 8$ K. The 3T2 was used for measuring the diffraction pattern of sample *A* at $T = 293$ and 8 K.

For samples *A*, *B*, and *C*, all diffraction lines corresponded to the well-known Hg-1201 structure with the tetragonal $P4/mmm$ space group. No attributes of extraneous phases were obtained, confirming the high quality of these samples. For sample *D*, weak peaks (intensities were less than 1% of the strongest peak) of the $\text{Ba}_2\text{CuO}_{3+x}$ phase were found in the spectrum.

Data processing was performed by the Rietveld method using the MRJA (Ref. 20) and FULLPROF (Ref. 21) programs for diffraction patterns from HRFD and 3T2, correspondingly. For the coherent scattering length, we used²² 12.69, 5.07, 7.718, and 5.803 fm (1 fm = 10^{-13} cm) for Hg, Ba, Cu, and O, respectively. The absorption correction was calculated using the tabulated absorption and incoherent scattering cross sections. For the HRFD spectra the influence of absorption was noticeable for $d \geq 1.8$ Å ($\lambda \geq 3.5$ Å). The lattice parameter calibration was done using the Al_2O_3 NIST standard SRM-676. Rietveld structural analysis of the HRFD spectra was performed on the d_{hkl} interval from 0.81 to 2.09 Å, with 110 diffraction peaks of Hg-1201, using the starting parameters as given in Ref. 3. Figure 2 shows an example of

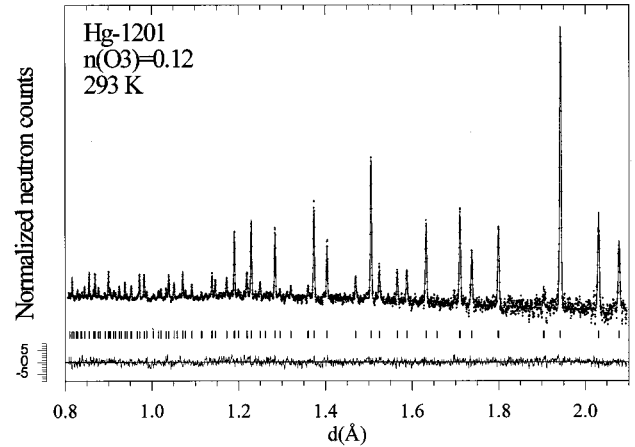


FIG. 2. Neutron-diffraction pattern of $\text{HgBa}_2\text{CuO}_{4.12}$ (sample *C*), measured at room temperature with the HRFD diffractometer. Experimental points, calculated profile, and difference curve are shown. The difference curve is normalized on the mean-square deviation.

these refinements ($\delta \approx 0.12$, sample *C*). The diffraction patterns measured on the 3T2 diffractometer were refined for the interval of $6^\circ \leq \theta \leq 126^\circ$ with ~ 150 peaks. The refinements were performed for the z coordinates of Ba and O2 (oxygen in the apical position), the occupancy factors of Hg and O3 (oxygen in the center of the Hg plane), and for the thermal factors of all atoms except the O3 atom. In the final refinement, the thermal factor of copper was kept fixed [$B(\text{Cu}) = 0.5$] to reduce the influence of systematic errors on the occupancy factor analysis.

IV. RESULTS AND DISCUSSION

A. Structure data for Hg-1201

The initial refinement was carried out assuming full occupancy of the mercury positions. The results are presented in Table II, together with the relevant bond distances. The good correspondence between the data for sample *A*, which were obtained on two diffractometers and by using different refinement programs, can be noted.

On the whole, the listed results are in good agreement with the Hg-1201 structure data published in Refs. 4–9, and especially with the data of a recent neutron-diffraction study.⁶ All of the known features of the Hg-1201 structure and, specifically, the dependence on temperature and oxygen content mentioned in Refs. 4–6, are confirmed.

The decrease in the a and c lattice parameters was 0.008 (0.009) and 0.025 (0.027) Å, respectively, for sample *A* (*B*) as the temperature decreased to 8 K. The shortening of the c axis in sample *A* is mainly the result of the shortening of the Cu-O2 bond distance, while both Cu-O2 and Hg-O2 distances decrease in the same degree in sample *B*.

For the samples with various extra oxygen contents, there is a correlation between δ and the value of the lattice parameters and some interatomic bonds. The Cu-O1 in-plane distance and the Cu-O2 apical distance decrease if δ increases, while the Hg-O2 distance increases (Fig. 3). The significant dependence of the Cu-O2 and Ba-O3 apical bonds on extra oxygen should be stressed. The overall contraction of the c

TABLE II. Structural parameters for $\text{HgBa}_2\text{CuO}_{4+\delta}$ obtained at room temperature and $T=8$ K with the HRFD and 3T2 diffractometers. The data are given after refinement with a fixed mercury occupancy factor, $n(\text{Hg})=1$. The results for $n(\text{Hg})$ and $B(\text{Hg})$ that were obtained in a joint refinement are also listed (3T2 data were processed by this variant only). All other structural parameters changed negligibly (smaller than their errors) whether $n(\text{Hg})$ was fixed or varied. Parameters without errors were fixed in the final refinement. The relevant interatomic and interlayer (denoted as l) distances (in Å) are also presented.

| Sample (T_c) Diffractom. Collected at | A (71 K) | | | B (83 K) | | C (98 K) | D (96 K) |
|---|---------------|--------------|------------|---------------|-------------|---------------|---------------|
| | HRFD 293 K | 3T2 293 K | 3T2 8 K | HRFD 293 K | HRFD 8 K | HRFD 293 K | HRFD 293 K |
| a , Å | 3.8864(1) | 3.8862(2) | 3.8783(2) | 3.8795(1) | 3.8705(1) | 3.8851(1) | 3.8851(1) |
| c , Å | 9.5316(3) | 9.5319(5) | 9.5073(4) | 9.5237(3) | 9.4968(3) | 9.5263(3) | 9.5202(3) |
| Hg, n | 1 | | | 1 | 1 | 1 | 1 |
| B , Å ² | 1.92(6) | | | 1.82(5) | 0.74(9) | 1.66(5) | 1.73(8) |
| Hg, n | 0.97(1) | 0.94(2) | 0.94 | 0.94(1) | 0.93(2) | 0.96(2) | 0.91(2) |
| B , Å ² | 1.77(12) | 1.04(8) | 0.22(6) | 1.45(6) | 0.23(12) | 1.45(11) | 1.09(15) |
| Ba, z | 0.3007(3) | 0.3004(4) | 0.3007(4) | 0.2976(3) | 0.2972(5) | 0.2982(3) | 0.2982(3) |
| B , Å ² | 0.90(7) | 0.6 | 0.1 | 0.44(5) | 0.3 | 0.46(6) | 0.29(7) |
| Cu, B , Å ² | 0.5 | 0.5 | 0.1 | 0.5 | 0.2 | 0.5 | 0.5 |
| O1, B , Å ² | 1.08(7) | 0.70(8) | 0.38(8) | 0.79(5) | 0.35(8) | 0.65(6) | 0.18(7) |
| O2, z | 0.2059(3) | 0.2066(4) | 0.2079(4) | 0.2090(3) | 0.2088(5) | 0.2074(3) | 0.2080(3) |
| B , Å ² | 1.76(6) | 1.53(8) | 0.67(7) | 1.79(6) | 0.90(7) | 1.69(6) | 1.60(7) |
| O3, n | 0.057(10) | 0.07(2) | 0.07 | 0.19(1) | 0.19 | 0.124(9) | 0.12(1) |
| B , Å ² | 1.0 | 1.0 | 0.5 | 1.0 | 0.5 | 1.0 | 1.0 |
| R_p | 0.068 | 0.057 | 0.068 | 0.058 | 0.056 | 0.070 | 0.095 |
| R_w | 0.068 | 0.071 | 0.085 | 0.059 | 0.056 | 0.065 | 0.077 |
| R_e | 0.086 | 0.066 | 0.077 | 0.062 | 0.071 | 0.088 | 0.116 |
| χ^2 | 1.065 | 1.18 | 1.21 | 1.78 | 1.06 | 1.07 | 1.13 |
| Cu-O2 | 2.803(3) | 2.797(4) | 2.777(4) | 2.771(3) | 2.765(5) | 2.787(3) | 2.780(3) |
| Hg-O2 | 1.963(3) | 1.969(4) | 1.977(4) | 1.990(3) | 1.983(5) | 1.975(3) | 1.980(3) |
| Cu-O1 | 1.9432 | 1.9431 | 1.9392 | 1.9398 | 1.9352 | 1.9426 | 1.9426 |
| Ba/ l -Cu/ l | 1.900(3) | 1.903(4) | 1.895(4) | 1.928(3) | 1.927(5) | 1.922(3) | 1.921(3) |
| Ba/ l -O2/ l | 0.904(4) | 0.894(5) | 0.882(5) | 0.844(4) | 0.840(7) | 0.865(4) | 0.859(4) |
| Ba-O3 | 2.866(3) | 2.863(4) | 2.859(4) | 2.834(3) | 2.822(5) | 2.834(3) | 2.839(3) |

lattice parameter is only 0.008 Å over a range of δ from $\delta \approx 0.06$ (sample A) to $\delta = 0.19$ (sample B), while both the Cu-O2 and Ba-O3 distances decrease by ~ 0.03 Å. As a result the interlayer distance between the Ba and O2 layers decreases greatly (by ≈ 0.06 Å). Qualitatively, this can be interpreted on the basis of the Coulomb splitting model, suggested in Ref. 23, as a positive charge transfer to the CuO_2 layer when the oxygen content increases in the HgO_δ layer.

B. Occupation of mercury positions

As shown in Table II, the temperature factors of Hg and O2, which form a dumbbell configuration of Hg-O₂ are quite large. The same unexpectedly large values of these parameters were found in Refs. 4–8. Thermal motion gives an essential contribution to the thermal factors, because at $T=8$ K, the value $B(\text{Hg})$, for instance, becomes several times smaller in comparison with room temperature, though it stays large. This last effect can indicate some structural disorder or partial occupation of the site. The attempt at structure refinement with disordered Hg sites gave no effect, which means that there is no static displacement. In a joint

refinement of Hg occupancy and thermal parameter the coordinates of other atoms do not change but $n(\text{Hg})$ and $B(\text{Hg})$ are markedly reduced (these new values are also listed in Table II). These two parameters, $n(\text{Hg})$ and $B(\text{Hg})$, correlate strongly that do not lead to a conclusion about their real values. In Fig. 4, the dependence of $n(\text{Hg})$ on $B(\text{Hg})$ is shown, which was obtained in a refinement at fixed values of $B(\text{Hg})$ for sample C. The same figure shows the R_w factor as a function of $B(\text{Hg})$, with a gently sloping minimum at $B(\text{Hg}) = 1.0 - 1.8$ Å² and, accordingly, at $n(\text{Hg}) = 0.9 - 1.0$.

A possible explanation for such a low occupancy factor or the large thermal factor of Hg can be mercury substitution for copper or a carbonate group, as it was suggested in Refs. 5, 7, and 8. If the condition $n(\text{Hg}) + n(\text{Cu}/\text{C}) = 1$ is fulfilled, the refined occupancy factors would be $n(\text{Hg}) \approx 0.9$ and $n(\text{Cu}/\text{C}) \approx 0.1$. The authors of Refs. 5 and 7 have proved the Hg substitution for Cu by the additional extra oxygen atoms located near the middle of the edge of the Hg mesh with an appropriate square coordination for the Cu cations. We tried to find this additional oxygen by calculating the experimental scattering density distribution and drawing maps for the various cross sections of the unit cell. The very high d_{hkl} reso-

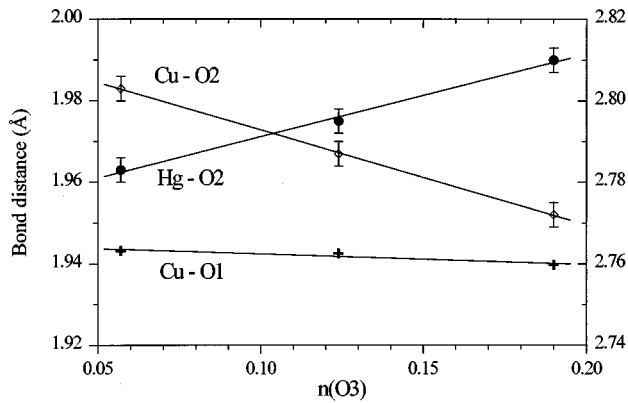


FIG. 3. Bond distances Cu-O2 (right scale), Cu-O1 and Hg-O2 (left scale) as a function of extra oxygen content δ . O1 is oxygen in the CuO_2 planes, O2 is apical oxygen.

lution of our diffraction patterns helped us to obtain the real F_{hkl} values for many of the diffraction peaks, which is very important in finding the low occupancy positions.

The sensitivity of the search can be estimated from Fig. 5, where the difference map of the scattering density for the basal plane of sample A with $\delta \approx 0.06$ is shown. The scattering density maximum of the O3 atom can be clearly seen. The amplitude of its peak is ~ 2.5 times larger than the most intensive background maxima. This means that atoms with coherent scattering lengths close to that of oxygen (for instance, carbon) would be found if occupation of their positions in the structure is close or higher than 3%. The $(1/2, y, z)$ cross section of the Fourier map for sample C is shown in Fig. 6. One can see that in the positions $1/2, 0, z$ ($z \approx 0.04$) and $1/2, y, 0$ ($y \approx 0.08$), where additional oxygen was found in Refs. 5 and 7, no real peaks are present. It

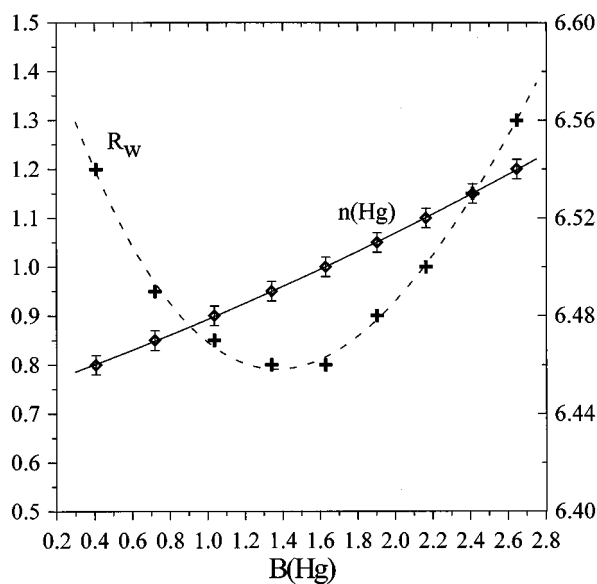


FIG. 4. Occupancy of the Hg position (0,0,0) as obtained in the refinement for sample C data at various fixed values of the thermal factor $B(\text{Hg})$ (left scale) and related values of the R_w factor (right scale, in %).

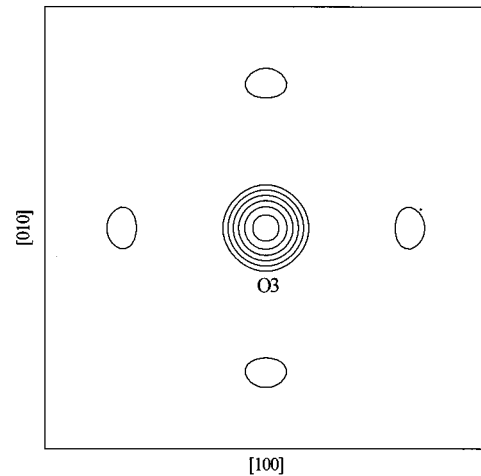


FIG. 5. The difference scattering-density map for the basal plane of sample A calculated with the difference of the experimental and calculated structure factors, $(F_{\text{expt}} - F_{\text{calc}})$. The O3 oxygen was excluded from the calculation of F_{calc} . The amplitude of the O3 maximum is equivalent to the coherent scattering length of 0.35 fm, the background peak amplitudes are not higher than 0.14 fm.

should be noted that we did not see any static disorder of the O3 atom along the diagonal that was found in Ref. 7.

Thus, the additional O4 atom and, consequently, the noticeable substitution of Hg for Cu were not present in our samples and we can now conclude that the large value of $B(\text{Hg})$ and $B(\text{O2})$ are the consequence of large oscillations of the HgO_2 fragment as a whole. It should be mentioned once more that the chemical analysis performed with one of our samples showed a practically stoichiometric cation composition and, consequently, confirmed an absence of noticeable cation replacement. The same conclusion was made in Ref. 6 on the basis of structural data, and in Ref. 24 where the studies of $\text{Hg}_{1-x}\text{Cu}_x\text{Ba}_2\text{CuO}_{4+\delta}$ samples obtained under high pressure of 1.8 GPa were carried out. This agrees also

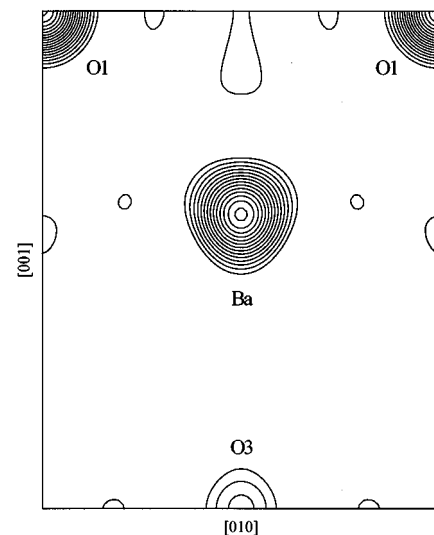


FIG. 6. Experimental scattering-density map (calculated with F_{expt} structure factors) of the $(x=0.5, 0 \leq y \leq 1, 0 \leq z \leq 0.5)$ plane of the unit cell of sample C ($\delta \approx 0.12$).

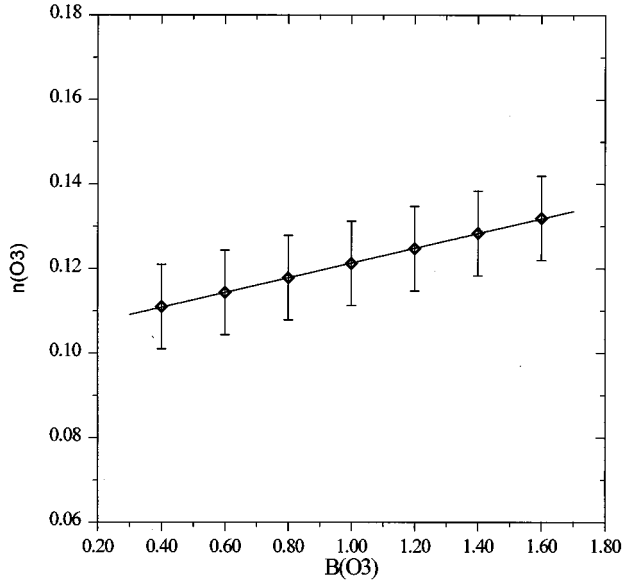


FIG. 7. The occupancy of the O3 position (1/2,1/2,0) as obtained in the refinement for the sample C data at various fixed values of the thermal factor $B(\text{O}3)$.

with the right temperature dependence of $B(\text{Hg})$ and $B(\text{O}2)$ although the x-ray-absorption fine-structure (XAFS) data²⁵ did not show large amplitudes of Hg-O bond movement, due to its high covalence.

The other additional effect that can raise the value of $B(\text{Hg})$ is the deficiency of Hg positions at the surface of the Hg-1201 grains, which was found in Ref. 26 for quenched samples. To some degree, this is proved by comparing the results obtained for samples C and D, which were synthesized at different oxygen partial pressures (0.15 and 0.0012 bar) and then annealed under the same conditions. The different oxygen partial pressures in a closed volume during the synthesis of Hg-1201 lead to the different mercury partial pressures, which was higher for sample D. This means that this sample should be more Hg deficient than sample C. Indeed, the c axes of these two samples are different, while the a parameters are the same. It is interesting to note that sample D has a lower T_c value that can also be a consequence of the cation stoichiometry violation.

C. Extra oxygen position occupation and its influence on T_c

Special attention was made to the extra oxygen O3 occupancy refinement. The small amount of extra oxygen in the structure does not allow its thermal parameter to be determined accurately. The problem is alleviated by the small correlation between O3 occupancy and thermal parameter. The variation of $B(\text{O}3)$ over a large range [parameter refinement with different fixed $B(\text{O}3)$ values] did not change δ more than one standard deviation (Fig. 7). The much stronger correlation shown in Fig. 4 was found between $n(\text{Hg})$ and $B(\text{Hg})$, but changing these values did not vary the δ value. Refinements done with and without the absorption correction caused an alteration of less than 0.01 for the δ value.

The $n(\text{O}3)$ parameters are listed in Table II, they were obtained with fixed $B(\text{O}3)=1 \text{ \AA}^2$. These occupancy param-

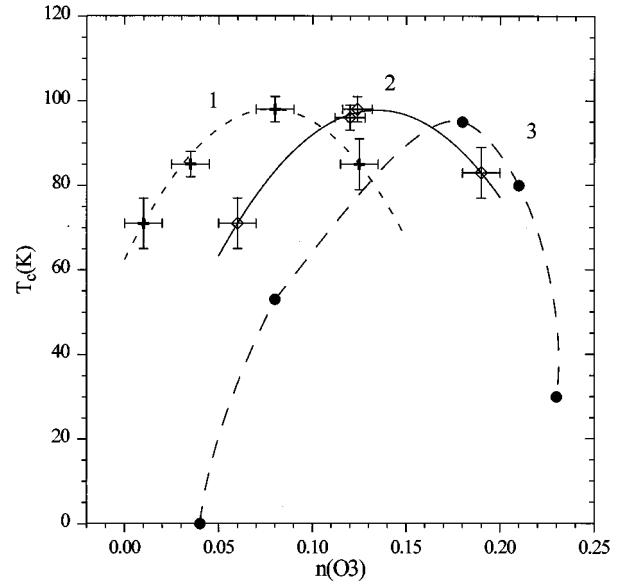


FIG. 8. The behavior of T_c vs δ drawn for our neutron-diffraction data (curve 2, \diamond) for samples A–D, together with data from Ref. 6 (curve 3, \bullet) and our data of iodometric titration (curve 1, $+$).

eters are significantly smaller than those determined by Huang *et al.*⁶ for the $\text{HgBa}_2\text{CuO}_{4+\delta}$ superconductors with close T_c 's (curves 2 and 3 in Fig. 8). A shift in the two $T_c(\delta)$ dependencies from each other with $\delta \approx 0.05$ can be easily seen. The $T_c(\delta)$ dependence for our samples where the δ content was determined by iodometric titration, assuming $V_{\text{Ba}}=V_{\text{Hg}}=+2$, $V_{\text{O}}=-2$ is shown also in Fig. 8. The additional experimental data obtained by this analysis for other Hg-1201 samples synthesized under similar conditions are depicted in Fig. 8 by the same sign (+).

The paraboliclike dependencies are shifted from each other along the δ axis. The maximum discrepancy in the δ values for the samples with close T_c 's exists between the iodometric data and the neutron-diffraction data from Ref. 6. The estimated hole concentration for the Hg-1201 sample with maximum T_c , based on thermoelectric power data was found to be +2.16 (Ref. 11) and it fits well with our iodometric data. However, the thermoelectric power technique allows only the hole concentration in the (CuO_2) layers to be estimated, while the iodometric titration determines the overall hole concentration and does not distinguish the holes between the different structural fragments: the (CuO_2) layers or the Hg or O atoms, etc. The discrepancies between the neutron-diffraction and thermoelectric power data were explained in Refs. 6 and 11 as that, for every extra oxygen inserted, one hole in the (CuO_2) layers is created while its formal charge becomes -1 . Self-consistent local-density-approximation calculations performed for the Hg-1223 structure revealed strong covalence between Hg and interstitial oxygen,²⁷ which decreases significantly the doping level of the (CuO_2) layers in comparison with that expected from formal ionic consideration. However, chemical analysis, which determines the overall hole concentration, in the case of the optimally doped Hg-1201 phase, must reveal the hole concentration $p=0.32$. Our experimental data for the samples with maximum T_c 's were much lower ($p=0.16$ or

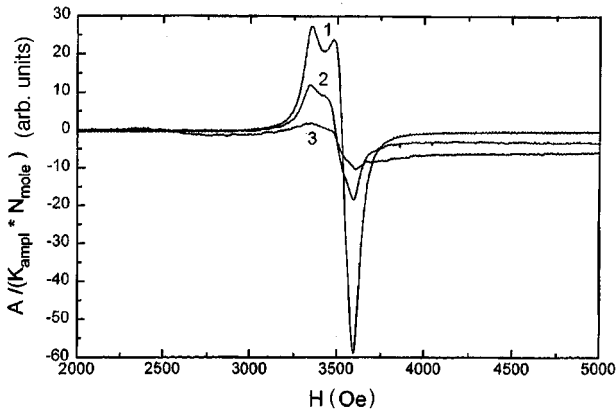


FIG. 9. The EPR spectra for samples A (curve 3) and C (curve 2). Curve 1 is the EPR spectra of the Y_2BaCuO_5 compound, reduced 1000 times.

$V_{Cu} = +2.16$), and this fact creates some doubts about the assumption of the O3 formal charge being equal to -1 .

The presence of the O^- anion in the Hg-1201 structure, located far from the cations, ($d_{Hg-O3} = 2.75 \text{ \AA}$ and $d_{Ba-O3} = 2.84 \text{ \AA}$) should provide a response in the EPR spectra due to the unpaired electron. The EPR spectra (first derivative of the absorption signal) normalized by the amplifier coefficient K_{amp} and the mole number N_{mole} of the reduced sample A and sample C treated in an oxygen flow are shown in Fig. 9. In the same figure, the 1000-times-reduced EPR spectrum of Y_2BaCuO_5 is shown. This structure has an unpaired electron in the Cu^{2+} cation and was used as a standard. All spectra exhibit large g -factor anisotropy: $g_{\perp} = 2.04 \pm 0.02$ and $g_{\parallel} = 2.23 \pm 0.02$, which is typical for powdered samples of compounds with Cu^{2+} cations in their structure in an axial-symmetric coordination.

Due to the low intensity of the EPR signals of the Hg-1201 samples, and practically the same line shape and width for all three of the samples studied, an estimation of the paramagnetic centre concentration was made using $A_{norm} = A/(K_{amp} \times N_{mole})$ and was compared with A_{norm} for Y_2BaCuO_5 . The values thus obtained (number of unpaired electrons per formula unit) are 3.5×10^{-4} for sample C and 1.4×10^{-4} for sample A. Such a small number of paramagnetic centers (more than 400 times smaller than the extra oxygen concentration) and a shape specific to the Cu^{2+} cations, the width of the signals and the values of the g factors, allow us to conclude that the EPR signals from the O^- anions are absent. However, this phenomenon can be attributed to the covalent interaction between Hg and extra oxygen, as it was revealed in Ref. 27. The origin of the weak EPR signals can be due to local defects in the Hg-1201 structure or to small amounts of impurity phases (not found by XRD analysis) containing Cu^{2+} cations.

Additional confirmation of the absence of O^- anions in the Hg-1201 structure is the much lower δ value obtained in Refs. 4 and 9 and in the present work in comparison with the data from Ref. 6. It should be noted that for the second member of the series, $HgBa_2CaCu_2O_{6+\delta}$,^{9,28,29} whose structure has one type of Cu cation in a pyramidal coordination, the optimal δ value as calculated for one (CuO_2) layer is also smaller and equals $\delta/2 = 0.11$ for all of the compounds studied.

V. CONCLUSIONS

The realized study of monophasic $HgBa_2CuO_{4+\delta}$ samples with different δ and T_c at the neutron high-resolution diffractometers allowed new precise structural information to be obtained, including thermal atomic parameters and extra oxygen concentration.

Scattering density maps were calculated to find the possible appearance of additional atoms in the Hg layer, with the exception of the O3 atom located in the middle of the mesh. We conclude that no significant replacement of Hg cations by others takes place and no additional extra oxygen atoms near the middle of the edge were found in our particular samples of the Hg-1201 phase. The large value of the temperature factors of Hg and O2, which form a dumbbell configuration of Hg-O₂, are the consequence of large oscillations of this fragment as a whole.

The determined $T_c(\delta)$ dependence exhibits a parabolic-like behavior similar to that found in previous works,^{6,8,10,11} and it agrees with the iodometric analysis data. However, these curves are shifted apart along the δ axis, an especially large shift is between the neutron-diffraction data from Ref. 6 and the iodometric data. The probable reason can be that despite the high accuracy of the neutron data [standard deviation of the $n(O3)$ is about 0.01], the real error can be significantly larger and cause a systematic shift from the real $n(O3)$ value. First of all, the large discrepancies in extra oxygen content can be due to distinct cation composition of Hg-1201 phases studied by different groups. In this case the T_c values are determined not only by oxygen content, but by a range of cations replacement also.

From our analysis, including the analysis of correlation between occupancy and thermal factor of the O3 atom, we believe that systematic error for oxygen content in our samples does not exceed 0.02. A small additional reason of δ shifting towards to a higher value can be extra oxygen inhomogeneity in the sample, leads to the polyphase state of a sample. Such phenomenon of macroscopic phase separation, due to low-temperature extra oxygen diffusion, was studied already in detail both for powdered samples³⁰ and single crystals³¹ of $La_2CuO_{4+\delta}$. The presence of incoherent scattering domains with different amounts of the extra oxygen in the crystallites of the sample can lead to a higher value of δ if the refinement was done using the single phase model. But, such effects cannot be strong. The 15% broadening of the reflections in the studied Hg-1201 samples, in comparison with the experimental resolution function of the diffractometer, supports the anion inhomogeneity hypothesis. In turn, the iodometric data may be shifted to smaller δ due to the possible presence of amorphous impurity phases in the sample.

Taken into account these factors, we can conclude that the optimal δ values for the Hg-1201 superconductor are in the range $\delta = 0.08 - 0.12$. The large discrepancy of our data with the δ values determined in Ref. 6 (where $\delta = 0.18$ was found) is not clear. The hypothesis of the O3 formal charge being equal to -1 causes some doubts and cannot explain this discrepancy. We think that the probable reason for overestimation of the O3 content can be due to the phenomena discussed above or due to an insertion of the additional "non-oxidizing" oxygen atoms into the structure, located in the

CO_3^{2-} groups, as was suggested in Ref. 8, or in the $\text{OH}^-(\text{H}_2\text{O})$ groups.

Additional neutron-diffraction experiments of monophasic Hg-based superconductors, especially with large amounts of extra oxygen, e.g., $\text{HgBa}_2\text{CaCu}_2\text{O}_{6+\delta}$, will allow important information to be obtained concerning the mechanism of hole creation in this superconducting series. The data obtained in the present work (neutron-diffraction, iodometry, EPR) support the traditional mechanism of hole creation in the conducting band, with a concentration close to 2δ .

ACKNOWLEDGMENTS

The authors are grateful to Professor H. G. von Schnering and O. Buresch (MPI-Stuttgart) for chemical analysis and Dr. P. E. Kazin (MSU) for magnetic measurements. This work was partly supported by INTAS (93-2483), the Russian Scientific Council on Superconductivity (Poisk-3), the Russian Science Foundation (93-02-2530), and NATO linkage grant (HTECH LG 951022).

- *Author to whom correspondence should be addressed: Frank Lab of Neutron Physics, JINR 141980 Dubna, Moscow reg. Russia.
- ¹E. V. Antipov and S. N. Putilin, *Priroda* (Moscow), **10**, 3 (1994).
 - ²I. Bryntse and S. N. Putilin, *Physica C* **212**, 223 (1993).
 - ³S. N. Putilin, E. V. Antipov, O. Chmaissem, and M. Marezio, *Nature* (London), **362**, 226 (1993).
 - ⁴O. Chmaissem, Q. Huang, S. N. Putilin, M. Marezio, and A. Santoro, *Physica C* **212**, 259 (1993).
 - ⁵J. L. Wagner, P. G. Radaelli, D. G. Hinks, J. D. Jorgensen, J. F. Mitchell, B. Dabrowski, G. S. Knapp, and M. A. Beno, *Physica C* **210**, 447 (1993).
 - ⁶Q. Huang, J. W. Lynn, Q. Xiong, and C. W. Chu, *Phys. Rev. B* **52**, 462 (1995).
 - ⁷A. Asab, A. R. Armstrong, I. Gameson, and P. P. Edwards, *Physica C* **255**, 180 (1995).
 - ⁸S. M. Loureiro, E. T. Alexandre, E. V. Antipov, J. J. Capponi, S. de Brion, B. Souletie, J. L. Tholence, M. Marezio, Q. Huang, and A. Santoro, *Physica C* **243**, 1 (1995).
 - ⁹M. Paranthaman and B. C. Chakoumakos, *J. Solid State Chem.* **121**, 221 (1996).
 - ¹⁰M. A. Subramanian (unpublished).
 - ¹¹Q. Xiong, Y. Y. Xue, Y. Gao, F. Chen, J. Gibson, L. M. Liu, A. Jacobson, and C. W. Chu, *Physica C* **251**, 216 (1995).
 - ¹²V. A. Alyoshin, D. A. Mikhailova, and E. V. Antipov, *Physica C* **255**, 173 (1995).
 - ¹³J. B. Torrance, Y. Tokura, A. I. Nazzari, A. Bezinge, T. C. Huang, and S. S. P. Parkin, *Phys. Rev. Lett.* **61**, 1127 (1988).
 - ¹⁴M. R. Presland, J. L. Tallon, R. G. Buckley, R. S. Liu, and N. E. Flower, *Physica C* **176**, 95 (1991).
 - ¹⁵S. D. Obertelli, J. R. Cooper, and J. L. Tallon, *Phys. Rev. B* **46**, 14 928 (1992).
 - ¹⁶A. F. Wells, *Structural Inorganic Chemistry*, 5th ed. (Clarendon Press, Oxford, 1984).
 - ¹⁷E. M. Koptin, E. V. Antipov, J. J. Capponi, P. Bordet, C. Chaillout, S. de Brion, M. Marezio, A. P. Bobylev, and G. Van Tendeloo, *Physica C* **243**, 222 (1995).
 - ¹⁸G. N. Mazo, V. M. Ivanov, and A. V. Kumkova, *Fresenius J. Anal. Chem.* **350**, 718 (1994).
 - ¹⁹V. L. Aksenov, A. M. Balagurov, V. G. Simkin, A. P. Bulkin, V. A. Kudryashev, V. A. Trounov, O. Antson, P. Hiismaki, and A. Tiitta, *J. Neutron Res.* (to be published).
 - ²⁰V. B. Zlokazov and V. V. Chernyshev, *J. Appl. Cryst.* **25**, 591 (1992).
 - ²¹J. Rodriguez-Carvajal, *Physica B* **192**, 55 (1993).
 - ²²V. F. Sears, *Neutron News* **3**, 26 (1992).
 - ²³S. Sh. Shilstein, A. S. Ivanov, and V. A. Somenkov, *Physica C* **245**, 181 (1995).
 - ²⁴E. T. Alexandre, S. M. Loureiro, E. V. Antipov, P. Bordet, S. de Brion, J. J. Capponi, and M. Marezio, *Physica C* **245**, 207 (1995).
 - ²⁵C. H. Booth, F. Bridges, E. D. Bauer, G. G. Li, J. B. Boyce, T. Claeson, C. W. Chu, and Q. Xiong, *Phys. Rev. B* **52**, R15 745 (1995).
 - ²⁶Y. Y. Xue, Q. Xiong, Y. Gao, I. Rusakova, Y. Y. Sun, and C. W. Chu, *Physica C* **255**, 1 (1995).
 - ²⁷D. J. Singh and W. E. Pickett, *Phys. Rev. Lett.* **73**, 476 (1994).
 - ²⁸P. G. Radaelli, J. L. Wagner, B. A. Hunter, M. A. Beno, G. S. Knapp, J. D. Jorgensen, and D. G. Hinks, *Physica C* **216**, 29 (1993).
 - ²⁹S. M. Loureiro, E. V. Antipov, J. L. Tholence, J. J. Capponi, O. Chmaissem, Q. Huang, and M. Marezio, *Physica C* **217**, 253 (1993).
 - ³⁰J. D. Jorgensen, B. Dabrowski, Shiyu Pei, D. G. Hinks, L. Soderholm, B. Morosin, J. D. Schirber, E. L. Venturini, and D. S. Ginley, *Phys. Rev. B* **38**, 11 337 (1989).
 - ³¹A. M. Balagurov, A. A. Zakharov, V. Yu. Pomjakushin, and V. G. Simkin, *Physica C* **272**, 277 (1996).